



Role of T2 mapping of magnetic resonance imaging in the differentiation of endometrial cancer and benign endometrial lesions

Han Xu
 Jie Zhang
 Yuqing Han
 Qingwei Liu
 Jinlai Liu
 Xianshun Yuan
 Jiamei Li
 Jinye Li
 Ximing Wang

From the Department of Radiology (H.X., J.Z. ✉ zhangjie1219@163.com, Y.H., Q.L.), Shandong Provincial Hospital, Cheeloo College of Medicine, Shandong University, Shandong, China; Department of Radiology (J.Z., Q.L., X.Y., X.W.), Shandong Provincial Hospital Affiliated to Shandong First Medical University, Shandong, China; Department of Radiology (J.L.), The Second People's Hospital of Jiaozuo (First Affiliated Hospital of Henan Polytechnic University), Jiaozuo, China; Department of Radiology (Jia.L.), Shandong Provincial Hospital Affiliated to Shandong First Medical University, Jinan, China; Department of Radiology (Jin.L.), Shandong Provincial ENT Hospital Affiliated to Shandong University, Shandong Provincial ENT Hospital, Jinan, China.

Received 24 August 2021; revision requested 25 September 2021; last revision received 28 March 2022; accepted 22 April 2022.



Epub: 28.12.2022

Publication date: 31.01.2023

DOI: 10.4274/dir.2021.21884

PURPOSE

The T2 mapping of magnetic resonance imaging (MRI) in endometrial cancer (EC), benign endometrial lesions (BELs), and normal endometrium (NE) has rarely been reported. This study aimed to determine the T2 values of MRI in EC, BELs, and NE to investigate whether the T2 values can differentiate them and to assess the aggressiveness of EC.

METHODS

In total, 73 patients [EC, 51 (age, 57.4 ± 5.4 years); BELs, 22 (age, 57.8 ± 11.8 years)] and 23 normal volunteers (age, 56.1 ± 6.6 years) were included. The T2 values of MRI of the EC (type I and II), BEL, and NE groups were described and compared. The relationships between the T2 values of MRI in EC and the pathological characteristics [International Federation of Gynecology and Obstetrics (FIGO) stage and grade] were analyzed.

RESULTS

The median T2 values of NE, BEL, and EC were 197.5 (142.9–324.0) ms, 131.1 (103.2–247.9) ms, and 103.0 (71.6–243.5) ms ($P < 0.001$), respectively. The median T2 values of type I and type II EC were 100.8 (71.62–130.44) ms and 125.7 (119.7–243.5) ms, respectively. There were significant differences in the T2 values among the NE, BEL, type I EC, and type II EC groups ($P < 0.001$) except for between the type II EC and BEL groups ($P = 0.938$). The T2 value of MRI in type I EC was significantly lower than that in type II EC ($P = 0.001$). There were no significant differences in patients with type I EC having different FIGO stages ($P = 0.273$) or tumor grades ($P = 0.686$).

CONCLUSION

T2 mapping of MRI has the potential to quantitatively differentiate between EC, BELs, and NE as well as between type I and type II EC.

KEYWORDS

Benign, benign endometrium lesions, endometrial cancer, MRI, T2 mapping, T2 value

Endometrial cancer (EC) is a common gynecologic malignancy and the sixth most prevalent cancer among women worldwide.¹ The risk factors for EC include conditions promoting increased estrogen exposure, such as hormonal replacement therapy, obesity, tamoxifen use, early menarche, late menopause, nulliparity, history of polycystic ovary disease, and hereditary no-polyposis colorectal cancer (Lynch syndrome).^{2,3} An accurate diagnosis of EC and an assessment of its aggressiveness are crucial for determining the treatment plan and prognosis of patients. Sampling is not always sufficient and not always possible (e.g., cervical stenosis after cervical radiation therapy).⁴ Psychologically, patients are more likely to accept non-invasive examinations. The pathologic type, stage, and grade of EC are important biological manifestations of its aggressiveness. Type II EC (non-estrogen-dependent EC) is closely linked with lymph node metastasis and poor prognosis. Many studies based on magnetic resonance imaging (MRI) have reported on the preoperative diagnosis and as-

assessment methods of EC.⁵⁻¹³ Techniques such as T2-weighted imaging (T2WI), dynamic contrast-enhanced (DCE) imaging, and diffusion-weighted imaging (DWI) are widely accepted, with high accuracy for the staging of EC.⁵⁻⁹ Other emerging techniques such as amide proton transfer (APT) imaging, magnetic resonance spectroscopy (MRS), and diffusion kurtosis imaging are also reported to have produced promising results regarding the type and grade of EC.¹⁰⁻¹³

Most of the studies on EC have focused on the application of qualitative MRI data. Meanwhile, quantitative MRI data could provide more unique and direct information regarding EC. The T2 value from MRI T2 mapping, which describes the decay of the magnetic vector (M) in the xy plane $[(M)_{xy}]$, a component of the total M, is an essential parameter in quantitative MRI. The T2 value reflects the absolute transversal relaxation time of the protons in the tissue. T2 mapping is mainly applicable for the musculoskeletal system, heart, and prostate because these tissues are composed of water compartments of different sizes, whose relative percentages vary between abnormal and normal tissues and between different pathologic grades of cancers.¹⁴⁻¹⁹

Few studies have reported on the application of T2 mapping in cases of normal uterine structure and uterine lesions. A short article reported that T2 mapping demonstrated a new layer, namely the linear submucosal myometrium of the uterine architecture, in one patient with adenomyosis and two patients with EC.²⁰ The difference in the myometrial architecture could partly be attributed to the difference in water content in the endometrium;²¹ the T2 value was related to the water content. To the best of our knowledge, no study focusing on T2 mapping for the differentiation of EC has been reported. This would require knowledge of the T2 values of MRI of the normal endometrium (NE) and benign endometrial lesions (BELs),

which have rarely been reported. This study aimed to determine the T2 values of MRI in EC, BELs, and NE to investigate whether the T2 values can differentiate them and to assess the aggressiveness of EC based on the T2 values.

Methods

Subjects

The Institutional Review Board of Shandong Provincial Hospital approved this prospective study (approval number: SWYX2020-051). Written informed consent was obtained from all subjects before enrollment.

Patients with a confirmed or suspected diagnosis of EC by diagnostic curettage, those who showed intrauterine lesions on ultrasound but had contraindications to curettage, and those who did not receive any surgical treatment other than curettage were included. Patients with lesions that could not be clearly visualized upon MRI were excluded. From March 2012 to September 2015, 51 patients with EC and 22 patients with BELs confirmed by histopathology were included in this study.

The T2 values of the endometrium may vary depending on the menstrual cycle, and as the majority of patients with EC and BELs were post-menopausal women, the volunteers with NE that were included in this study were also post-menopausal women;²² hence, the influence of menstrual cycle was not a consideration in the T2 values of MRI in the volunteers with NE. These volunteers were required to have no clinical symptoms, no submucous myoma on MRI, and no other gynecological diseases. Any volunteers with gynecological abnormalities after five years of follow-up were excluded. Finally, 23 volunteers with NE were included in this study.

Image acquisition

MRI was performed using a 3T scanner (Magnetom Verio, Siemens Healthineers, Erlangen, Germany). Built-in integrated spine coils and an eight-channel pelvic phased array surface coil were used to receive signals. Patients were advised to fast for 4 h and were administered a raceanisodamine hydrochloride injection (Hangzhou Minsheng Pharma, Hangzhou, China) before MRI to reduce intestinal peristalsis, and their bladder was required to be partially full.

For anatomical scans, oblique sagittal, oblique coronal and oblique axial T2W turbo spin-echo (TSE) imaging, oblique axial and oblique sagittal DWI, and oblique sagittal DCE imaging were performed using the following parameters: oblique axial, sagittal, and coronal T2WI, repetition time (TR)/echo time (TE), 2,950–3,670/97–101 ms; slice thickness (ST)/gap, 3–4 (0.6–0.8) mm; average, 2; matrix, 320 × 256 or 320 × 310; field of view (FOV), 20 × 20 cm; oblique axial and sagittal DWI, TR/TE, 6,200/93 ms; ST/gap, 3–4 (0.6–0.8) mm; average, 6; matrix, 160 × 120; FOV, 20 × 20 cm; oblique sagittal DCE imaging, TR/TE, 5.21/1.8 ms; ST/gap, 3–4 (0.6–0.8) mm; average, 1; matrix, 224 × 161; FOV, 20 × 20 cm.

Oblique sagittal T2 mapping was performed using multi-echo TSE prior to DCE imaging, with the following parameters: TR, 1,500 ms; TE, 20, 40, 60, 80 and 100 ms; FOV, 20 × 20 cm; matrix, 256 × 256; ST, 3 mm; slice gap, 0.6 mm; 12 slices. The saturated band was placed on the anterior abdominal wall with an acquisition time of 4 m and 8 s.

Image analysis

The T2 map was analyzed using the vendor's workstation (Syngo, Siemens Healthineers, Erlangen, Germany). The T2 mappings from the 23 normal volunteers and 73 patients were reviewed in consensus by two senior gynecologic radiologists (Zhang J and Xu H) who had 8 and 10 years of experience in clinical practice, respectively. On oblique sagittal T2 maps, the region of interest (ROI) was manually delineated along the edge of a lesion in consensus by the two radiologists according to the morphology and size of a lesion to avoid cystic and necrotic areas (Figure 1). A larger lesion contained more than one ROI. The ROI was drawn on each slice containing the lesion. The three-dimensional volume of interest (VOI) was constructed by the multiple two-dimensional ROIs. The ROI and VOI of NE were manually drawn in the same manner (Figure 2). The multi-parametric MR images, including DWI, DCE, and T2W images, were used as references to avoid cystic or necrotic areas. The ROI of EC and BELs were drawn with DCE images as the main reference, while the ROI of NE was drawn with T2W images as the main reference. The VOI of NE often contained more than one ROI. The mean T2 value of a VOI was calculated by averaging the T2 values of all voxels in a VOI

$$\text{mean T2} = (\sum_{i=1}^n T2_i S_i) / \sum_{i=1}^n S_i, \text{ equation 1}$$

Main points

- The T2 mapping of magnetic resonance imaging in endometrial cancer (EC), benign endometrial lesions (BELs), and normal endometrium (NE) has rarely been reported.
- T2 mapping can help differentiate between EC, BELs, and NE.
- T2 mapping cannot differentiate between type II EC and BELs.
- T2 mapping cannot differentiate between the different stages or grades of EC.

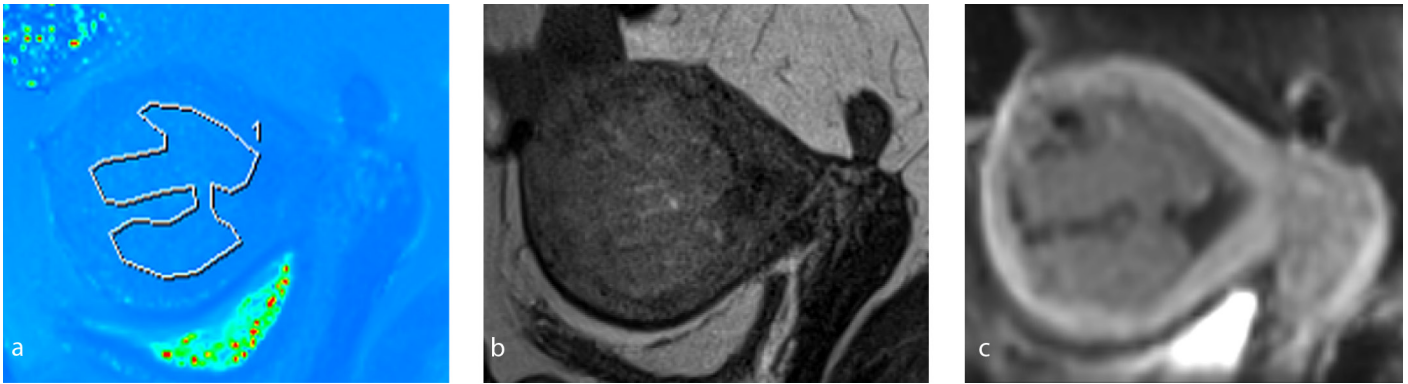


Figure 1. The ROI in a 65-year-old woman with type II endometrial cancer. (a) The ROI was manually placed in the lesions on the sagittal T2 map according to the morphology and size of the lesions to avoid the cystic and necrotic areas; (b) sagittal T2-weighted image and (c) sagittal enhanced image were used as the reference images. ROI, region of interest.

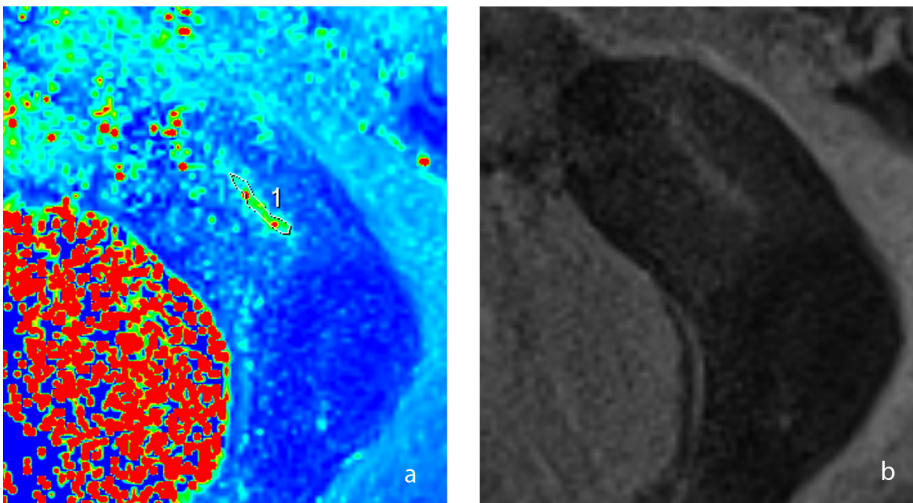


Figure 2. The ROI of normal endometrium in one slice in a 70-year-old volunteer. (a) T2 map of normal endometrium "1" was the ROI. (b) T2-weighted image was used as the reference image. ROI, region of interest.

where n was the number of ROIs for a lesion/NE (that is a VOI), T_{2_i} was the mean T2 value of the i th ROI, and S_i was the area of the i th ROI. As the area between each ROI in a lesion/NE is different, the area S_i was the weighting of the T_{2_i} to robustly calculate the mean T2 values.

After the measurement of the T2 values (in consensus by the two radiologists) for more than six months, the values were independently measured by a manually placed ROI by the two radiologists for interclass reliability analysis. Two weeks later, the T2 values were repeatedly measured by one of the two radiologists for intraclass reliability analysis.

Histopathological analysis

The median interval between MRI and surgery was 3 (1–10) days. In total, 51 patients with EC underwent total hysterectomy and bilateral salpingo-oophorectomy and pelvic lymph node dissection, 19 patients with BELs underwent total hysterec-

tomy and bilateral salpingo-oophorectomy, and 3 patients with BELs (2 with complex hyperplasia and 1 with simple hyperplasia) underwent resection of the lesions. The lesions were histopathologically analyzed by a senior pathologist (Li J). Following the International Federation of Gynecology and Obstetrics (FIGO) 2009 revised FIGO staging criteria,²³ the stage, histologically differentiated degree (grade 1, well differentiated; grade 2, moderate differentiation; grade 3, poor differentiation), and type (type I, estrogen-dependent; type II, non-estrogen-dependent) of EC were reported.

Statistical analysis

The Kolmogorov–Smirnov test was used to check the data normality. If the distribution was normal, values were represented as the mean \pm standard deviation; otherwise, the median and minimum–maximum values were given. Descriptive statistics of categorical variables were expressed as fre-

quency and percentage [n (%)]. Intra- and interobserver agreements of T2 values were analyzed by reliability analysis. If the data fit the normal distribution and the homogeneity of variance (Levene test), a one way analysis of variance (ANOVA) was used for the intergroup comparisons; otherwise, the Kruskal–Wallis H test was used. If the Kruskal–Wallis H test was statistically significant, the Dunn–Bonferroni post hoc test was used for pairwise comparisons. The corrected $P < 0.05$ was considered statistically significant.

The receiver operating characteristic (ROC) curve analysis was performed, and the optimal threshold of the T2 value to distinguish between the two types of EC was obtained from the ROC curve analysis, according to the Youden index. The area under the curve (AUC) was of great significance in the comprehensive evaluation of diagnostic accuracy. In general, $0.5 < AUC \leq 0.7$ indicated a low diagnostic value, $0.7 < AUC \leq 0.9$ indicated an intermediate diagnostic value, and $AUC > 0.9$ indicated a high diagnostic value.¹¹

Few patients had type II EC in this study, which included multiple pathological types. Therefore, the following statistical analysis was only performed for type I EC. The T2 values of MRI in the different FIGO stages of EC as well as for the different grades of EC were compared. Spearman's correlation coefficient was used in the analysis of the relationship between the FIGO stage of type I EC and the T2 value as well as between the grade of type I EC and the T2 value. For all statistical analyses, $P < 0.05$ was considered significant. The statistical analysis was performed using IBM SPSS statistics 22.0 for Windows (IBM Corp, Armonk, NY, USA).

Results

The mean ages of the 51 patients with EC, 22 patients with BELs, and 23 normal volunteers (NE) were 57.4 ± 5.4 years, 57.8 ± 11.8 years, and 56.1 ± 6.6 years, respectively. There were no significant differences between the ages of patients with EC, BELs, and NE ($P = 0.743$). The cases of EC included 4 (7.8%) premenopausal patients (mean age, 49.8 ± 1.3 years) and 47 (92.2%) post-menopausal patients (mean age, 58.0 ± 5.2 years). The cases of BEL included 4 (18.2%) premenopausal patients (mean age, 39.8 ± 8.8 years) and 18 (81.8%) post-menopausal patients (mean age, 61.8 ± 8.1 years).

The characteristics of the patients and volunteers are summarized in Table 1. The intra- and interclass correlation coefficients of the T2 values were 0.981 [$P < 0.001$, 95% confidence interval (CI), 0.971, 0.987] and 0.949 ($P < 0.001$, 95% CI, 0.894, 0.972), respectively. The T2 values of MRI in patients with EC, BELs, and NE are shown in Table 2. There were statistically significant differences in the T2 values between EC, BELs, and NE ($P < 0.001$; EC vs. BEL, $P = 0.001$; EC vs. NE, $P < 0.001$; BEL vs. NE, $P = 0.005$) (Table 2, Figure 3a).

The T2 values of MRI in patients with type I and type II EC are also shown in Table 2. There were significant differences in the T2 values

Table 1. Patient characteristics	
Variable	n (%)
Lesions	
EC	51/96 (53.1)
BELs	22/96 (22.9)
NE	23/96 (24.0)
Type of EC	
Type I (estrogen-dependent)	41/51 (80.4)
Type II (non-estrogen-dependent)	10/51 (19.6)
Subtype of type II EC	
Adenosquamous	2/10 (20.0)
Squamous cell	2/10 (20.0)
Endometrioid	2/10 (20.0)
Serous	2/10 (20.0)
Mucinous	1/10 (10.0)
Mixed endometrioid/clear cell	1/10 (10.0)
Subtype of BELs	
Polyp	7/22 (31.8)
Complex hyperplasia with or without atypia	9/22 (40.9)
Simple hyperplasia	6/22 (27.3)
nN, number; EC, endometrial cancer; BELs, benign endometrial lesions; NE, normal endometrium.	

between patients with type I EC, type II EC, BELs, and the volunteers with NE ($P < 0.001$). There was no significant difference in the T2 values between type II EC and BELs ($P = 0.938$); however, there were statistically significant differences in the T2 values between all other pairs of groups (NE vs. BEL, $P = 0.006$; NE vs. type I EC, $P < 0.001$; NE vs. type II EC, $P = 0.006$; BEL vs. type I EC, $P < 0.001$; type I EC vs. type II EC, $P = 0.001$) (Figure 3b). The AUC of differentiation between the two types of EC was 0.959 ($P < 0.001$), i.e., a high diagnostic value (Figure 4a, Table 3). The threshold of the T2 value was 119.3 ms. The Youden index, specificity, and sensitivity were 0.902, 0.902, and 1.000, respectively. The AUC of differentiation between type I EC and BEL was 0.920 ($P < 0.001$) (Figure 4b, Table 3). The threshold of the T2 value was 119.3 ms. The Youden index, specificity, and sensitivity were 0.675, 0.773, and 0.902, respectively.

The clinical information and results of the T2 mapping analysis of patients with type I EC are shown in Table 4. There were no significant differences in the patients with type I EC having different FIGO stages ($P = 0.273$

or different tumor grades ($P = 0.686$) (Table 4). Because there was only one case of EC in FIGO stage II, the EC cases in FIGO stages II and III were combined for statistical analysis. There was no significant correlation between the T2 value and FIGO stage of EC (Spearman coefficient $r_1 = 0.176$, $P = 0.271$) or between the T2 value and grade of EC (Spearman coefficient $r_2 = 0.228$, $P = 0.152$). No patient with type II EC had cancer of FIGO stage Ia. The mean T2 values for type II EC with the FIGO stage Ib (two patients) and stage II (two patients) were 123.4 ms and 125.7 ms, respectively. Six patients with type II EC had cancer of FIGO stage III; the median (minimum–maximum) value was 134.8 (119.7–243.5) ms. As very few patients had type II EC, statistical analysis of the different FIGO stages was not performed.

Discussion

This study demonstrated that the T2 values of MRI in patients with NE, BELs, and EC were significantly different. The T2 value of MRI in patients with BELs was significantly lower than in those with NE, while the T2 val-

Table 2. T2 values of MRI in volunteers with NE and patients with BELs and EC

Cases	Median (min–max)	Kruskal–Wallis test <i>P</i> -value	Pairwise <i>P</i> -value
NE	197.5 (142.9–324.0)	<0.001	NE vs. BEL, 0.005
BEL	131.1 (103.2–247.9)		BEL vs. EC, 0.001
EC	103.0 (71.6–243.5)		EC vs. NE, <0.001
NE	197.5 (142.9–324.0)	<0.001	NE vs. BEL, 0.006
BEL	131.1 (103.2–247.9)		NE vs. type I EC, <0.001
Type I EC	100.8 (71.62–130.44)		NE vs. type II EC, 0.006
Type II EC	125.7 (119.7–243.5)		BEL vs. type I EC, <0.001
			BEL vs. type II EC, 0.938
			Type I vs. type II EC, 0.001

MRI, magnetic resonance imaging; NE, normal endometrium; BELs, benign endometrial lesions; EC, endometrial cancer; min, minimum value; max, maximum value.

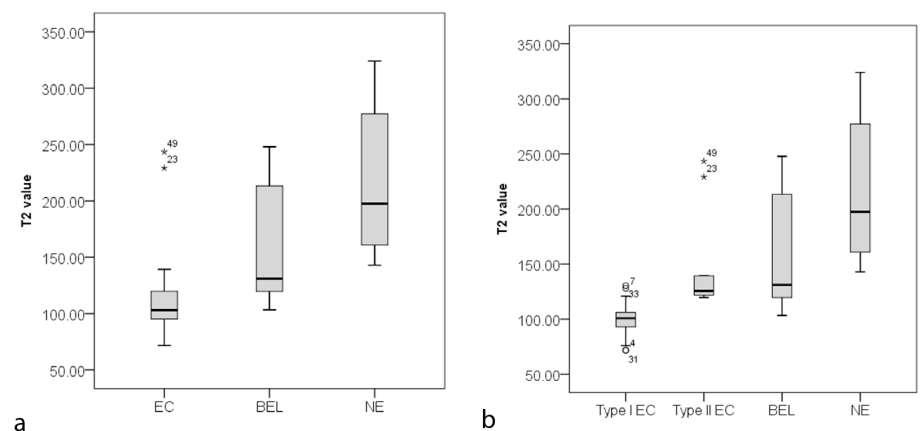


Figure 3. Box plot of the T2 value of MRI in patients with EC, BELs, and NE. (a) There were statistically significant differences between the T2 values in patients with EC, BEL, and NE. (b) There were statistically significant differences between all pairs of groups, except for between patients with type II EC and BELs. Two patients had serous cancer with a relatively high T2 value (*). MRI, magnetic resonance imaging; EC, endometrial cancer; BELs, benign endometrial lesions; NE, normal endometrium.

ue in patients with EC, specifically type I EC, was significantly lower than in patients with BELs. Women with NE have normal secretion function and their glands are arranged in proper order. The acinar cavity and tissue space of the NE are relatively large, thereby accommodating more secretions and interstitial fluids. Hence, the T2 value of MRI is highest for those with NE. Patients with EC and BELs have different degrees of gland heteromorphism, especially those with EC. The EC has a high nucleus: plasma ratio, obvious nucleolus, and irregular glandular lumen.^{24,25}

Hence, the T2 values of MRI in patients with EC and BELs are reduced to different degrees.

Furthermore, the T2 value of MRI in patients with type II EC was higher than that in patients with type I EC. However, the T2 values of MRI at different FIGO stages of EC were not significantly different; a similar finding was noted in patients with different grades of EC. Unfortunately, there was no significant difference in the T2 values of MRI between patients with type II EC and BELs. Type II EC has many pathological types, in-

cluding serous cancer, which is characterized by the secretion of more serous fluid. In this study, only two patients with type II EC had serous cancer (Figure 3), and they had relatively high T2 values of MRI. In such cases, benign and malignant lesions should be distinguished first using other MRI sequences such as DWI and contrast-enhanced imaging.²⁶ A previous study has shown that the apparent diffusion coefficient (ADC) of EC is lower than that of BEL, the b1000q of EC was higher than that of BEL, and the Cq of EC was lower than that of BEL (b1000q = DWI signal-intensity lesion/DWI signal-intensity myometrium; Cq = postcontrast signal-intensity lesion/postcontrast signal-intensity myometrium).²⁶

It is vital to distinguish EC from BELs before initiation of treatment. Fractional dilatation and curettage (D & C) is the most commonly used method for preoperative diagnosis of EC; however, it does not always yield reliable results because of the limited number of samples.⁴ About 16.7% to 62.5% of patients diagnosed with atypical hyperplasia during D & C were diagnosed as having EC based on the hysterectomy specimens.¹¹ Occasionally, the results of D & C are inconsistent with those of the hysterectomy specimens, and a certain rate of false negative results with D & C has also been observed.²⁷ Further, hysteroscopic fractional D & C may cause the spread of tumor cells within the peritoneal cavity.²⁸ Conventional qualitative MRI may some-

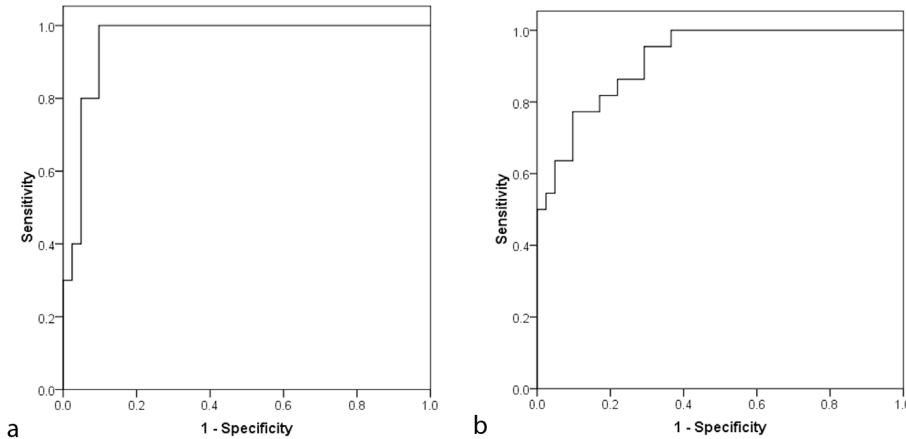


Figure 4. (a) The ROC curve to differentiate type II EC from type I EC. The area under the curve was 0.959, with a high diagnostic value. The Youden index was 0.902, with a sensitivity of 1 and a specificity of 0.902. (b) The ROC curve to differentiate type I EC from BELs. The area under the curve was 0.920, with a high diagnostic value. The Youden index was 0.675, with a sensitivity of 0.902 and a specificity of 0.773. ROC, receiver operating characteristic; EC, endometrial cancer; BELs, benign endometrial lesions.

	T2 value cut-off (ms)	Sensitivity	Specificity	AUC	SE	P value
Type I - II	119.3	1	0.902	0.959	0.026	<0.001
Type I - BELs	119.3	0.773	0.902	0.920	0.033	<0.001

EC, endometrial cancer; BELs, benign endometrial lesions; AUC, area under the curve; SE, standard error.

Variable	T2 value (ms)		n (%)
	Mean ± SD	Median (min-max)	
Type I EC			41/51 (80.4)
FIGO stage			
Ia	-	98.7 (75.8-120.4)	24/41 (58.5)
Ib	-	105.5 (90.1-130.4)	10/41 (24.4)
≥II	-	103.0 (71.6-120.8)	7/41 (17.1)
P-value	0.273		
Grade			
Grade 1	98.0 ± 7.2	-	8/41 (19.5)
Grade 2	99.9 ± 16.2	-	27/41 (65.9)
Grade 3	104.4 ± 7.4	-	6/41 (14.6)
P value	0.686		

EC, endometrial cancer; SD, standard deviation; n, number; min, minimum value; max, maximum value; FIGO, International Federation of Gynecology and Obstetrics.

times render the differentiation of EC from BELs difficult.²² In this study, the T2 values of MRI in patients with EC were significantly lower than those in patients with BELs. Thus, this quantitative MRI parameter might be a supplement to preoperative pathological examination and routine MRI.

Considerable differences exist between the different types of EC in terms of histology, risk factors, and clinical features as well as in terms of therapeutic schedule, risk of surgery, and recurrence rate.²⁹ Type I EC is the most common, accounting for 80% to 85% of all EC, and it has a favorable prognosis, whereas type II EC is characterized by rapid tumor progression and a poor prognosis. Typically, the diagnosis of the different types of EC (estrogen-dependent or non-estrogen-dependent) depends on postoperative immunohistochemical examination rather than preoperative and intraoperative pathological examinations.³⁰ In the current study, the T2 value of MRI in type I EC was significantly lower than that in type II EC, which might help to distinguish between the two types of EC before surgery.

Recent studies have reported that some quantitative parameters could distinguish EC from benign lesions and identify the different types of EC and different FIGO stages of EC. A previous study by Zhang et al.¹¹ reported that the mean [choline-containing compounds (Cho)]/water obtained from MRS could distinguish EC from benign lesions and identify the different types of EC; they found that Cho/water was positively correlated with the FIGO stage of EC. Takayama et al.¹⁰ found that the APT signal intensity was positively correlated with the histologic grade of EC. Nougaret et al.⁹ reported that a combination of the volume and ADC of a tumor can be used to predict tumor grade, lymphovascular invasion, and depth of myometrial invasion. Some studies have reported on the MRI findings of type I to type II EC differentiation.^{31,32} Chen et al.³¹ reported that type II EC has a lower ADC and larger size than type I EC. Meng et al.³² reported that the magnetization transfer ratio asymmetry (3.5 ppm) and apparent kurtosis coefficient values were higher and the non-Gaussian diffusion coefficient was lower in type II EC than in type I EC. Most endometrial polyp lesions were iso/hypointense in the DWI sequence ($b = 1.000 \text{ s/mm}^2$), while the endometrium (endometrial physiological thickening) and endometrial hyperplasia lesions were hyperintense in the DWI sequence; there was no statistically significant difference between the endome-

trium (endometrial physiological thickening) and endometrial hyperplasia and polyp in ADC and Cq.²⁶ On T2WI, endometrial hyperplasia appeared iso/hypointense to the NE; however, T2WI appearance is non-specific.³³ The T2 value of NE was significantly higher than that of BELs in this study.

Ghosh et al.²⁰ reported that the T2 map can show the uterus with four layers. The thin fourth layer was more hypointense than the junctional zone and was observed between the endometrium and the junctional zone. T2* mapping can also show the fourth layer.³⁴ Quantitative T2 values seem to be suitable for distinguishing between prostate cancer and normal gland tissue or benign prostate hyperplasia nodes, and they offer an indication of the aggressiveness of the prostate cancer.^{14,18} To the best of our knowledge, no study has reported on the association between the invasiveness of EC and the T2 values of MRI. The T2 mapping techniques help to overcome the relatively insensitive visual inspection of differences in signal intensities. They allow direct measurement of T2 relaxation time in milliseconds and quantify the voxel-wise signal on a standardized scale, thereby enabling more direct investigation of the water content in the tissue and further tissue characterization. In this study, we investigated EC using T2 mapping and obtained some significant results.

This study has some limitations. First, the number of patients in this study was small, especially patients with type II EC, which included mostly uncommon histological types of EC, such as serous EC; therefore, more patients with type II EC are required for further research. Second, the normality of the endometrium of the healthy volunteers could only be assumed based on their clinical manifestations, imaging manifestations, and disease history; it could not be confirmed by histological examination as this was not considered ethical. Third, the T2 mapping was very sensitive to the water content in the endometrium. The area of interest could not be completely removed in case of slight endometrial secretions, which increase the T2 value, influencing the results. Fourth, the control group included only post-menopausal women; the same was not true for the patient group, which could have introduced some variation in the results. Fifth, T2 mapping is a difficult technique to reproduce, and a lot of variation exists in the parameters used to obtain T2 maps; in addition, there are no recommendations or standard values to achieve uniformity between studies. Last,

there was a high proportion of grade 2 lesions in patients with type I EC.

In conclusion, the present study shows that the differences in the T2 values between BELs and type II EC are not statistically significant. However, the T2 mapping of MRI has the potential to quantitatively differentiate between EC, BELs, and NE as well as between type I and type II EC.

Funding

The study was funded by Primary Research & Development Plan of Shandong Province (no. 2016GSF201095).

Conflict of interest disclosure

The authors declared no conflicts of interest.

References

1. Lortet-Tieulent J, Ferlay J, Bray F, Jemal A. International patterns and trends in endometrial cancer incidence, 1978-2013. *J Natl Cancer Inst.* 2018;110(4):354-361. [\[CrossRef\]](#)
2. Otero-García MM, Mesa-Álvarez A, Nikolic O, et al. Role of MRI in staging and follow-up of endometrial and cervical cancer: pitfalls and mimickers. *Insights Into Imaging.* 2019;10(1):19. [\[CrossRef\]](#)
3. Rizzo S, Femia M, Buscarino V, et al. Endometrial cancer: an overview of novelties in treatment and related imaging keypoints for local staging. *Cancer Imaging.* 2018;18(1):45. [\[CrossRef\]](#)
4. Zhu HL, Liang XD, Wang JL, Cui H, Wei LH. Hysteroscopy and directed biopsy in the diagnosis of endometrial carcinoma. *Chin Med J (Engl).* 2010;123(24):3524-3528. [\[CrossRef\]](#)
5. Beddy P, O'Neill AC, Yamamoto AK, Addley HC, Reinhold C, Sala E. FIGO staging system for endometrial cancer: added benefits of MR imaging. *Radiographics.* 2012;32(1):241-254. [\[CrossRef\]](#)
6. Nougaret S, Lakhman Y, Vargas HA, et al. From staging to prognostication: achievements and challenges of MR imaging in the assessment of endometrial cancer. *Magn Reson Imaging Clin N Am.* 2017;25(3):611-633. [\[CrossRef\]](#)
7. Park SB, Moon MH, Sung CK, Oh S, Lee YH. Dynamic contrast-enhanced MR imaging of endometrial cancer: optimizing the imaging delay for tumour-myometrium contrast. *Eur Radiol.* 2014;24(11):2795-2799. [\[CrossRef\]](#)
8. Wu LM, Xu JR, Gu HY, Hua J, Haacke EM, Hu J. Predictive value of T2-weighted imaging and contrast-enhanced MR imaging in assessing myometrial invasion in endometrial cancer: a pooled analysis of prospective studies. *Eur Radiol.* 2013;23(2):435-449. [\[CrossRef\]](#)

9. Nougaret S, Reinhold C, Alsharif SS, et al. Endometrial Cancer: Combined MR volumetry and diffusion-weighted imaging for assessment of myometrial and lymphovascular invasion and tumor grade. *Radiology*. 2015;276(3):797-808. [\[CrossRef\]](#)
10. Takayama Y, Nishie A, Togao O, et al. Amide proton transfer MR imaging of endometrioid endometrial adenocarcinoma: association with histologic grade. *Radiology*. 2018;286(3):909-917. [\[CrossRef\]](#)
11. Zhang J, Cai S, Li C, et al. Can magnetic resonance spectroscopy differentiate endometrial cancer? *Eur Radiol*. 2014;24(10):2552-2560. [\[CrossRef\]](#)
12. Yue W, Meng N, Wang J, et al. Comparative analysis of the value of diffusion kurtosis imaging and diffusion-weighted imaging in evaluating the histological features of endometrial cancer. *Cancer Imaging*. 2019;19(1):9. [\[CrossRef\]](#)
13. Hori M, Kim T, Onishi H, et al. Endometrial cancer: preoperative staging using three-dimensional T2-weighted turbo spin-echo and diffusion-weighted MR imaging at 3.0 T: a prospective comparative study. *Eur Radiol*. 2013;23(8):2296-2305. [\[CrossRef\]](#)
14. Mai J, Abubrig M, Lehmann T, et al. T2 Mapping in prostate cancer. *Invest Radiol*. 2019;54(3):146-152. [\[CrossRef\]](#)
15. Kijowski R, Blankenbaker DG, Munoz Del Rio A, Baer GS, Graf BK. Evaluation of the articular cartilage of the knee joint: value of adding a T2 mapping sequence to a routine MR imaging protocol. *Radiology*. 2013;267(2):503-513. [\[CrossRef\]](#)
16. Nebelung S, Sondern B, Oehrl S, et al. Functional MR imaging mapping of human articular cartilage response to loading. *Radiology*. 2017;282(2):464-474. [\[CrossRef\]](#)
17. Puntmann VO, Isted A, Hinojar R, Foote L, Carr-White G, Nagel E. T1 and T2 mapping in recognition of early cardiac involvement in systemic sarcoidosis. *Radiology*. 2017;285(1):63-72. [\[CrossRef\]](#)
18. Sabouri S, Chang SD, Savdie R, et al. Luminal water imaging: a new MR imaging T2 mapping technique for prostate cancer diagnosis. *Radiology*. 2017;284(2):451-459. [\[CrossRef\]](#)
19. Hoang Dinh A, Melodelima C, Souchon R, et al. Quantitative analysis of prostate multiparametric MR images for detection of aggressive prostate cancer in the peripheral zone: a multiple imager study. *Radiology*. 2016;280(1):117-127. [\[CrossRef\]](#)
20. Ghosh A, Singh T, Bagga R, Srinivasan R, Singla V, Khandelwal N. T2 relaxometry mapping in demonstrating layered uterine architecture: parameter optimization and utility in endometrial carcinoma and adenomyosis: a feasibility study. *Br J Radiol*. 2018;91(1081):20170377. [\[CrossRef\]](#)
21. McCarthy S, Scott G, Majumdar S, et al. Uterine junctional zone: MR study of water content and relaxation properties. *Radiology*. 1989;171(1):241-243. [\[CrossRef\]](#)
22. Shitano F, Kido A, Kataoka M, et al. MR appearance of normal uterine endometrium considering menstrual cycle: differentiation with benign and malignant endometrial lesions. *Acta Radiol*. 2016;57(12):1540-1548. [\[CrossRef\]](#)
23. Creasman W. Revised FIGO staging for carcinoma of the endometrium. *Int J Gynaecol Obstet* 2009;105(2):109. [\[CrossRef\]](#)
24. Hendrickson M, Ross J, Eifel P, Martinez A, Kempson R. Uterine papillary serous carcinoma: a highly malignant form of endometrial adenocarcinoma. *Am J Surg Pathol*. 1982;6(2):93-108. [\[CrossRef\]](#)
25. Le Gallo M, O'Hara AJ, Rudd ML, et al. Exome sequencing of serous endometrial tumors identifies recurrent somatic mutations in chromatin-remodeling and ubiquitin ligase complex genes. *Nat Genet*. 2012;44(12):1310-1315. [\[CrossRef\]](#)
26. Bakir B, Sanli S, Bakir VL, et al. Role of diffusion weighted MRI in the differential diagnosis of endometrial cancer, polyp, hyperplasia, and physiological thickening. *Clin Imaging*. 2017;41:86-94. [\[CrossRef\]](#)
27. Eddib A, Allaf B, Lee J, Yeh J. Risk for advanced-stage endometrial cancer in surgical specimens from patients with complex endometrial hyperplasia with atypia. *Gynecol Obstet Invest*. 2012;73(1):38-42. [\[CrossRef\]](#)
28. Polyzos NP, Mauri D, Tsioras S, Messini CI, Valachis A, Messinis IE. Intraperitoneal dissemination of endometrial cancer cells after hysteroscopy: a systematic review and meta-analysis. *Int J Gynecol Cancer*. 2010;20(2):261-267. [\[CrossRef\]](#)
29. Huss A, Ihorst G, Timme-Bronsert S, Hasenburg A, Oehler MK, Klar M. The Memorial Sloan Kettering Cancer Center Nomogram is More Accurate than the 2009 FIGO Staging System in the Prediction of Overall Survival in a German Endometrial Cancer Patient Cohort. *Ann Surg Oncol*. 2018;25(13):3966-3973. [\[CrossRef\]](#)
30. Phelippeau J, Canlorbe G, Bendifallah S, et al. Preoperative diagnosis of tumor grade and type in endometrial cancer by pipelle sampling and hysteroscopy: Results of a French study. *Surg Oncol*. 2016;25(4):370-377. [\[CrossRef\]](#)
31. Chen J, Fan W, Gu H, et al. The value of the apparent diffusion coefficient in differentiating type II from type I endometrial carcinoma. *Acta Radiol*. 2021;62(7):959-965. [\[CrossRef\]](#)
32. Meng N, Wang X, Sun J, et al. Evaluation of amide proton transfer-weighted imaging for endometrial carcinoma histological features: a comparative study with diffusion kurtosis imaging. *Eur Radiol*. 2021;31(11):8388-8398. [\[CrossRef\]](#)
33. Pintican R, Bura V, Zerunian M, et al. MRI of the endometrium - from normal appearances to rare pathology. *Br J Radiol*. 2021;94(1125):20201347. [\[CrossRef\]](#)
34. Imaoka I, Nakatsuka T, Araki T, et al. T2* relaxometry mapping of the uterine zones. *Acta Radiol*. 2012;53(4):473-477. [\[CrossRef\]](#)